Structural Properties of Screened Coulomb Balls

M. Bonitz,[1] D. Block,[2] O. Arp,[2] V. Golubnychiy,[1] H. Baumgartner,[1] P. Ludwig,[1] A. Piel,[2] and A. Filinov[1]

[1]*ITAP, Christian-Albrechts-Universität zu Kiel, D-24098 Kiel, Germany*

[2]*IEAP, Christian-Albrechts-Universität zu Kiel, D-24098 Kiel, Germany*

(Received 23 August 2005; published 21 February 2006)

Small three-dimensional strongly coupled charged particles in a spherical confinement potential arrange themselves in a nested shell structure. By means of experiments, computer simulations, and theoretical analysis, the sensitivity of their structural properties to the type of interparticle forces is explored. While the normalized shell radii are found to be independent of shielding, the shell occupation numbers are sensitive to screening and are quantitatively explained by an isotropic Yukawa model.

DOI: 10.1103/PhysRevLett.96.075001 PACS numbers: 52.27.Lw, 52.27.Gr, 52.35.Fp, 82.70.Dd

The recently discovered Coulomb balls [1] are an interesting new object for studying strongly coupled systems. Coulomb balls consist of hundreds of micrometer sized plastic spheres embedded in a gas plasma. The plastic spheres attain a high electric charge Q of the order of several thousand elementary charges and arrange themselves into a highly ordered set of nested spherical shells with hexagonal order inside the shells. Coulomb balls are a special form of 3D-plasma crystals [2–4]. The formation of ordered clusters with nested shells was also observed in laser-cooled trapped ion systems, e.g., [5,6], and is expected to occur in expanding neutral plasmas [7,8].

The same kind of ordering was found in molecular dynamics (MD) simulations, e.g., [9–11], and references therein. In particular, the transition to the macroscopic limit [12,13], the symmetry properties of the individual shells including a Voronoi analysis [10] and metastable intrashell configurations [11,14] have been analyzed. Very large systems of trapped ions show a transition to the crystal structure of bulk material, which was measured by laser scattering [15].

Although the shell structure of ion crystals is quite well understood in terms of simulation results, these systems do not yet allow for systematic experimental studies of the structure inside the shells and the detailed occupation numbers of individual shells. The advantage of studying Coulomb balls is the immediate access to the full three-dimensional structure of the nested shell system by means of video microscopy. The tracing of each individual particle is ensured by the high optical transparency of the system, which results from particle diameters of typically 5 μm at interparticle spacings of 500 μm. Compared to atomic particles, the very high mass of the microparticles used here slows down all dynamic phenomena to time scales ranging from 10 ms to seconds. Therefore, studies of Coulomb balls complement investigations of ion crystals, where dynamical studies are difficult.

Coulomb balls are in a strongly coupled state, i.e., the Coulomb coupling parameter, $\Gamma = Q^2/ak_BT$, where a is the mean interparticle distance, attains large values ($\Gamma \gg 100$). Contrary to ion crystals, where the particles interact via the pure Coulomb force, the microparticles in a Coulomb ball are expected to interact by a Yukawa type pair potential, $V_{dd} = (Q^2/r)e^{-r/\lambda_D}$, which was verified experimentally in complex plasmas [16]. Therefore, Coulomb balls are characterized by two parameters, the coupling parameter Γ and the Debye shielding length of the plasma λ_D. It is the intention of this paper to study the influence of shielding on the structure of Coulomb balls, in particular, to pin down the differences from systems with pure Coulomb interaction. This will be done by comparing computer simulations with experimental results. At the same time, a study of spherical crystals with Yukawa interaction opens up an interesting new field which in a natural way bridges the gap between the above mentioned theoretical investigations of finite size Coulomb systems and the theory of macroscopic Yukawa plasmas, e.g. [17,18].

Experiment.—The experiment is described in detail in Refs. [1,14,19], so here we only summarize the main results from a systematic investigation of 43 Coulomb balls consisting of 100 to 500 monodisperse and hence uniformly charged particles. All Coulomb balls were trapped under identical experimental conditions. All of them had a spherical shape and their diameter was in the range of 4–5 mm. A typical experimental result for a cluster and its shell structure is shown in the left part of Fig. 1. In all 43 Coulomb balls a similar shell structure was observed and the shell radii R_s and the shell occupation numbers N_s were measured. Further, from the pair correlation function the typical mean interparticle distance was derived, which for all N was close to $a \simeq 0.6$ mm. The mean intershell distance d was found to be $d = (0.86 \pm 0.06)a$, which is in good agreement with local icosahedral ordering [9]. An important experimental result is that the intershell distance is constant over the whole Coulomb ball and implies a constant average density of particles and ions, which is equivalent to a parabolic electric potential well used for the simulations below. A more detailed experimental verification of the parabolic confinement well is described else-

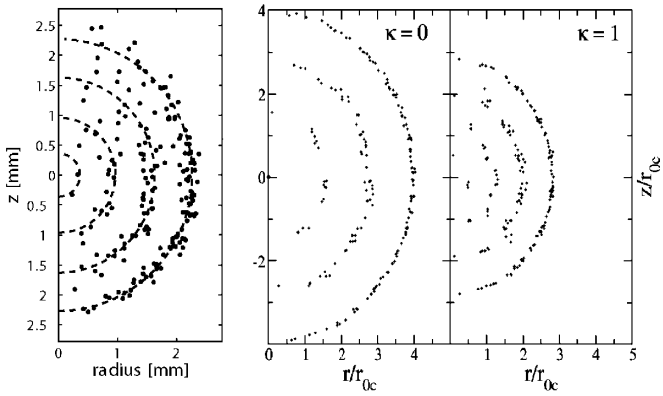

FIG. 1. Radial particle distribution for $N = 190$ given in cylindrical coordinates. Left: experiment [1], right two figures: MD-simulation results with Coulomb ($\kappa = 0$), and Yukawa ($\kappa = 1$) potential. The shell occupation numbers are compiled in Table I.

where [19]. A different case with ''self-confinement'' of a dust cloud in a strongly anharmonic potential was recently discussed in [20].

Simulations.—For a theoretical explanation of the experimental results we have performed molecular dynamics and thermodynamic Monte Carlo (MC) simulations using the Hamiltonian

$$H = \sum_{i=1}^{N}\left\{\frac{p_i^2}{2m} + U_c(\mathbf{r}_i)\right\} + \frac{1}{2}\sum_{i\neq j} V_{dd}(\mathbf{r}_i - \mathbf{r}_j). \qquad (1)$$

We assume that the Coulomb balls consist of particles with the same mass and charge and that a stationary state is reached close to thermodynamic equilibrium. Furthermore, the observed isotropic particle configuration suggests to use an isotropic interaction potential. Screening effects are included in static approximation using Debye(Yukawa)-type pair potentials V_{dd} given above. In the simulations we use dimensionless parameters, with lengths given in units of the ground state distance of two particles, r_{0c}, defined in Eq. (2), hence in this Letter $\kappa = r_{0c}/\lambda_D$. In experimental papers, $\kappa = a/\lambda_D$ is often used. In accordance with the experiment on Coulomb balls [19] and previous experiments and simulations on ion crystals [17], we use a screening-independent confinement potential $U_c(r) = m\omega^2 \cdot r^2/2$. As a result, in our model the configuration of the Coulomb balls is determined by three parameters: particle number N, screening parameter κ, and temperature T. Since experimental plasma densities and temperatures are not precisely known, we have performed a series of calculations for different values of κ and T. Furthermore, a wide range of particle numbers, up to $N = 503$, has been analyzed.

Results.—Consider first the theoretical ground state configurations ($T = 0$) in the case of Coulomb interaction, $\kappa = 0$, which were obtained by classical MD simulations using an optimized simulated annealing technique [11]. Using about 1000 independent runs for each value of N ensured that the ground state is reached. In addition, we have performed MC simulations in the canonic ensemble with a standard Metropolis algorithm, which allows for a rigorous account of finite temperature effects. Both simulations yield identical configurations at low temperature. Figure 1 shows a comparison of MD simulation and experiment for the case of $N = 190$ particles. In both cases four concentric spherical shells are observed, which are the result of a balance between confinement potential U_c and interparticle repulsion V_{dd}.

For a more detailed quantitative comparison between experiment and simulation we analyze the dependence of the shell radii R_s on the cluster size N (Fig. 2). The interparticle distance a serves as a common length scale as it is accessible in experiment and simulation. There is an overall increase $\propto N^{1/3}$ of the experimental R_s for all shells and all 43 analyzed clusters. Exceptions occur around values of N where new shells emerge. The same behavior is obtained from the MD simulations. Without any free parameter a very good agreement of experimental radii and Coulomb MD results (full lines) is observed, in particular, concerning the absolute values, the slope and the equidistance of the shells. Further, these results hold also in case of a Yukawa potential if κ is small (dashed lines in Fig. 2). Interestingly, the general scaling of the shell radii in units of the interparticle distance a of weakly shielded Coulomb balls $\propto N^{1/3}$ is the same as for pure Coulomb systems, such as ion crystals.

However, a marked difference between experiment and simulations of pure Coulomb systems is observed for the shell population numbers $N_1 \ldots N_4$. Table I shows the shell population numbers for various screening parameter κ of a Coulomb ball with $N = 190$ as obtained from MD simulations and experiment. Clearly, for $\kappa = 0$ the MD results yield systematically more particles in the outer part of the cluster than observed in experiment. Further, Table I shows that, with increasing κ, particles move from the outer shell

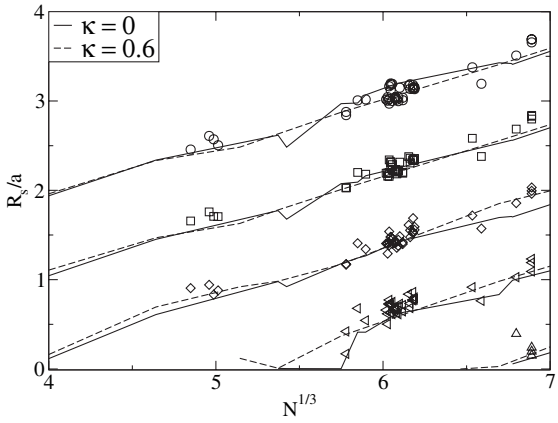

FIG. 2. Experimental (symbols) and MD-simulation (lines) results for the shell radii of three-dimensional Coulomb balls in units of the mean interparticle distance.

TABLE I. Experimental (last column) and theoretical shell configuration of the Coulomb ball $N = 190$. $N_1 \ldots N_4$ denote the particle numbers on the ith shell beginning in the center.

$\kappa \rightarrow$	0	0.2	0.3	0.4	0.5	0.6	1.0	Experiment
N_1	1	1	2	2	2	2	4	2
N_2	18	18	20	20	21	21	24	21
N_3	56	57	57	58	58	60	60	60
N_4	115	114	111	110	109	107	102	107

inward. Interestingly, for $\kappa = 0.58 \ldots 0.63$, the simulations yield exactly the same shell configuration as the experiment. Therefore, the different population numbers may be attributed to the influence of screening and hence weakening of the interaction potential.

To investigate this in more detail, the comparison was extended to all 43 Coulomb balls. Because of their different size and even different number of shells the systematic differences in shell population of Coulomb and Yukawa systems can be studied comparing the experimental results and MD simulations. The result is shown in Fig. 3. Coulomb and Yukawa simulations as well as the experiment reveal an almost linear behavior of the shell population of all shells as a function of $N^{2/3}$. However, the experimentally obtained population of the outermost shell N_4 is significantly smaller than the one of a Coulomb system (solid line), whereas the inner shells show a systematically higher population. Interestingly, the Yukawa MD simulations (dashed lines) show the same systematic deviation from the Coulomb case. It is clearly found that with increasing κ particles move to inner shells. Hence, the finding discussed for the Coulomb balls with $N = 190$ in Table I holds generally. This tendency reflects the fact that, from an energetic point of view, the higher population of the inner shells becomes less costly, due to the shielding

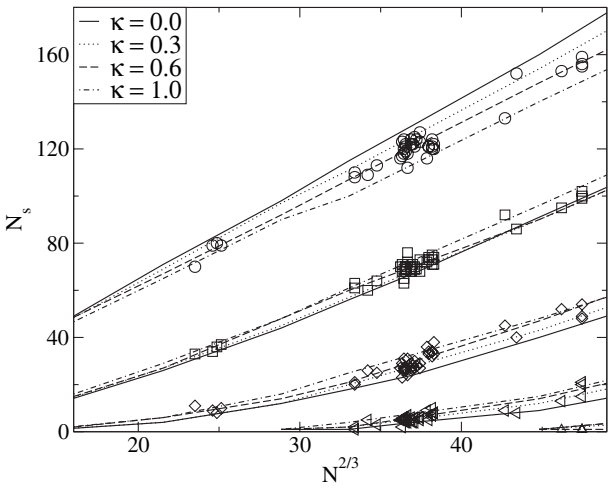

FIG. 3. Experimental (symbols) and simulation (lines) results for the shell population of three-dimensional Coulomb clusters at different values of κ (see inset).

than the occupation of the outermost shell, where the confinement by the trap dominates the potential energy.

In more detail, we find that the outermost shell exhibits the largest absolute change with κ and it is, therefore, best suited for a detailed comparison with the experimental data, see Fig. 3. From a best fit to the experimental data, we find a screening parameter $\kappa^{\mathrm{EXP}} = 0.62 \pm 0.23$. An independent analysis for the other shells confirms this result, e.g., the third shell, yields $\kappa^{\mathrm{EXP}} = 0.58 \pm 0.43$. Determining the mean interparticle distance a from the first peak of the pair distribution function κ^{EXP} translates into an average Debye length $\lambda_D/a = 1.54 \pm 0.7$. Furthermore, as one can see in the right hand part of Fig. 1, an increase of κ leads to compression of the entire cluster, which is due to the reduction of the potential V_{dd}. The fact that more and more particles move from the outer shells inward has the consequence that closed shell configurations are already reached at a smaller number N^* of total particles compared to N_c^* in the Coulomb case. While for $\kappa = 0$, the first closed shell is found at $N_1^* = 12$ particles, for $\kappa \gtrsim 4.7$ the ground state of a cluster with 12 (and 11 as well) particles contains one particle in the center and $N_1^* = 10$. For $\kappa = 0.6$ closure of the 2nd to 4th shell is observed for $N_2^* = 54$, $N_3^* = 135$, $N_4^* = 271$, whereas in the Coulomb case $N_{2c}^* = 57, 60$ [10], $N_{3c}^* = 154$ [14] and $N_{4c}^* = 310$ cf. also Fig. 2.

After analyzing the shell populations we now consider the shell width. The larger roughness of the shells in the experiments cf. Fig. 1, is attributed to small anisotropies of the experimental confinement and finite depth resolution of the imaging equipment as well as temperature effects. While the measurements are at room temperature, the MD simulations refer to $T = 0$. Therefore, we have analyzed the influence of temperature on the shell radii and populations with the help of MC simulations. From the results we conclude that the effect of temperature on the shell configurations N_s is negligible for $\kappa = 0.6$. At constant finite T we find that an increase of κ leads to a reduction of shell roughness. Contrary to that, a temperature increase at elsewhere fixed parameters in fact leads to a roughening of the shells proportional to $\sqrt{T}$ for the outer shell and an even stronger effect for the inner shells. This tendency will become evident from the analytical results below.

Analytical results.—The main influence of screening on Coulomb balls is readily understood with the help of analytical results, which can be found for $N = 2$. First, the ground state distance $r_0(\kappa)$ follows from minimizing the potential energy U in Eq. (1):

$$\frac{e^{\kappa r_0} r_0^3}{1 + \kappa r_0} = \frac{Q^2}{m/2\omega^2} \equiv r_{0c}^3. \tag{2}$$

Equation (2) yields the two-particle distance, r_{0c}, in an unscreened system as a function of r_0 and is easily inverted numerically [21]. The ratio r_0/r_{0c} is always smaller than

unity and monotonically decreasing with κ, thereby confirming the above observation of screening-induced compression of the Coulomb balls. Second, we analyze the cluster stability by expanding the potential U in terms of small fluctuations, $y \equiv r - r_0$, around the ground state, up to second order: $U(r) - U(r_0) = \frac{1}{2}U''(r_0)y^2 \equiv \frac{m}{4}\Omega^2 y^2$. This defines an effective local trap frequency Ω

$$\Omega^2(\kappa) = 3\omega^2\left(1 + \frac{1}{3}\frac{\kappa^2 r_0^2}{1 + \kappa r_0}\right) = \frac{6}{m}\frac{Q^2}{r_0^3} f_2(\kappa),$$
$$f_2(\kappa) = e^{-\kappa r_0}(1 + \kappa r_0 + \kappa^2 r_0^2/3), \tag{3}$$

which allows us to estimate the width of the Coulomb ball shells. Third, we compute the variance of the particle distance fluctuations, σ_r, for particles in a parabolic potential with frequency Ω at temperature T and obtain $\sigma_r^2 = 2k_B T/(m\Omega^2)$ which is in agreement with our MC simulations. This allows for two interesting conclusions: At constant screening, the shell width grows with temperature as $\sqrt{T}$ while screening reduces the shell width. One might be tempted to conclude that increased screening makes particle transitions between neighboring shells less likely and thus stabilizes the cluster against melting. However, the opposite is true, because screening also reduces the distance between shells which is of the order of r_0. The relative importance of both tendencies can be discussed in terms of the *relative distance fluctuations*, a critical value of which determines the onset of radial melting (Lindemann criterion).

$$u_r^2 \equiv \frac{\sigma_r^2}{r_0^2} = \frac{1}{3}\frac{1}{\Gamma_2^*}, \qquad \Gamma_2^* = \Gamma_2 f_2(\kappa). \tag{4}$$

u_r is related to an effective coupling parameter, Γ_2^* which depends on the interaction strength of two trapped particles—via the Coulomb-type coupling parameter, $\Gamma_2 \equiv Q^2/(k_B T r_0)$, and on the screening strength—via the function $f_2(\kappa)$. f_2 monotonically decreases with κ (u_r increases), thus *screening destabilizes the Coulomb balls*.

Finally, these analytical results are closely related to those for macroscopic homogeneous Yukawa systems, e.g. [17,18]. This limit is recovered by replacing, in (3), r_0 by the mean interparticle distance a at a given density n, $a = (3/4\pi n)^{1/3}$. Then the local trap frequency becomes $\Omega^2 \to \omega_{pd}^2 f_2(\kappa)$, showing that, in a Coulomb system, Ω approaches the dust plasma frequency ω_{pd} whereas, in the case of screening, the result is modified by a factor $\sqrt{f_2(\kappa)}$ [22]. Also, the effective coupling parameter Γ_2^* is in full analogy to the macroscopic result [18].

In summary, we have presented a combined experimental, numerical, and theoretical analysis of small spherical charged particle clusters. The excellent experimental accessibility of these systems has been demonstrated. The structure of these clusters deviates from models with pure Coulomb interaction and requires the inclusion of static screening. For the particle number range $N = 100 \ldots 500$, comparison with the MD and MC simulations has allowed us to determine the screening parameter averaged over the clusters as $\lambda_D/a \approx 1.5$. These Coulomb balls are representative for finite Yukawa systems, combining shell properties observed in spherical Coulomb clusters with screening effects found in Yukawa plasmas. Since the shell occupation numbers have now been critically analyzed, our results confirm earlier conclusions about the shell structure of ion clusters, where such an analysis was not accessible yet. The results are relevant for other strongly correlated charged particle systems, such as crystal formation of droplets in expanding laser produced plasmas, where shielding becomes important.

This work is supported by the Deutsche Forschungsgemeinschaft via SFB-TR 24 Grants A3, A5, and A7 and, in part, by DLR under Contract No. 50WM0039. We acknowledge discussions with W. D. Kraeft and M. Kroll's assistance in conducting the experiments.

[1] O. Arp, D. Block, A. Piel, and A. Melzer, Phys. Rev. Lett. **93**, 165004 (2004).
[2] J. B. Pieper, J. Goree, and R. A. Quinn, Phys. Rev. E **54**, 5636 (1996).
[3] M. Zuzic *et al.*, Phys. Rev. Lett. **85**, 4064 (2000).
[4] Y. Hayashi, Phys. Rev. Lett. **83**, 4764 (1999).
[5] D. J. Wineland *et al.*, Phys. Rev. Lett. **59**, 2935 (1987).
[6] M. Drewsen *et al.*, Phys. Rev. Lett. **81**, 2878 (1998).
[7] T. Pohl, T. Pattard, and J. M. Rost, Phys. Rev. Lett. **92**, 155003 (2004).
[8] T. Killian, Nature (London) **429**, 815 (2004).
[9] R. W. Hasse and V. V. Avilov, Phys. Rev. A **44**, 4506 (1991).
[10] K. Tsuruta and S. Ichimaru, Phys. Rev. A **48**, 1339 (1993).
[11] P. Ludwig, S. Kosse, and M. Bonitz, Phys. Rev. E **71**, 046403 (2005).
[12] H. Totsuji *et al.*, Phys. Rev. Lett. **88**, 125002 (2002).
[13] J. P. Schiffer, Phys. Rev. Lett. **88**, 205003 (2002).
[14] O. Arp *et al.*, J. Phys.: Conf. Ser. **11**, 234 (2005).
[15] W. M. Itano *et al.*, Science **279**, 686 (1998).
[16] U. Konopka, G. E. Morfill, and L. Ratke, Phys. Rev. Lett. **84**, 891 (2000).
[17] D. H. E. Dubin and T. M. O'Neill, Rev. Mod. Phys. **71**, 87 (1999).
[18] V. E. Fortov *et al.*, Phys. Rev. Lett. **90**, 245005 (2003).
[19] O. Arp, D. Block, M. Klindworth, and A. Piel, Phys. Plasmas **12**, 122102 (2005).
[20] H. Totsuji, C. Totsuji, T. Ogawa, and K. Tsuruta, Phys. Rev. E **71**, 045401 (2005).
[21] A useful analytical approximation for r_0 in Eq. (2) as a function of r_{0c} is $x = x_c + (\ln(1 + x_c) - x_c)/(x_c^2 + 3x_c + 3)[x_c(1 + x_c)]$, where $x = \kappa r_0$, which has an error of less than 1%, for $x_c = \kappa r_{0c} < 1.5$.
[22] This result differs slightly from the exact macroscopic result [18] (by the coefficient $1/3$ instead of $1/2$ in the last term in f_2) which is a consequence of performing this replacement in the two-particle expression (2).